JOURNAL OF GUIDANCE, CONTROL, AND DYNAMICS
Vol. 34, No. 2, March–April 2011

Improved Computation of Balancing Transformations for Aeroservoelastic Models via Time Scale Conversion

Daniel C. Hammerand,* James M. Gariffo,† and Kevin M. Roughen‡
M4 Engineering, Inc., Long Beach, California 90807

DOI: 10.2514/1.51071

Design of modern control laws motivates the creation of state-space models from aeroservoelastic models. Balanced truncation is often used to create reduced-order models. In the present work, a reduced-order model that employs a change in time scale in computing the balancing transformation is developed. The transformation matrix necessary to transform the original aeroservoelastic model is found from the aeroservoelastic model employing the recast time scale. Results from an aeroservoelastic wing and a supersonic transport model are shown, and it is demonstrated that, with an appropriate choice of time scale, the methodology results in greatly improved conditioning for the Lyapunov equations used to find the Gramians employed in the balancing transformation.

Nomenclature

$[A]$ = aeroservoelastic state matrix using the original time scale
$[\tilde{A}]$ = aeroservoelastic state matrix using the recast time scale
$[\bar{A}]$ = aeroservoelastic state matrix for the balanced system (original time scale)
$[a]$ = matrix of actuator delay constants
$[A_A]$ = aerodynamic state matrix
$[A^0]$ = constant term in Roger's rational function approximation
$[A^1]$ = linear term in Roger's rational function approximation
$[A^2]$ = quadratic term in Roger's rational function approximation
$[B]$ = aeroservoelastic input matrix using the original time scale
$[\tilde{B}]$ = aeroservoelastic input matrix using the recast time scale
$[\bar{B}]$ = aeroservoelastic input matrix for the balanced system (original time scale)
$\{\hat{B}_A\}$ = $N_l \times 1$ vector fully populated with values of 1.0
$[B_A^1]$ = aerodynamic input matrix corresponding to velocity input
$[B^l]$ = curve fit term corresponding to aerodynamic lag term l in Roger's rational function approximation
$[C]$ = aeroservoelastic output matrix using the original time scale
$[\tilde{C}]$ = aeroservoelastic output matrix using the recast time scale
$[\bar{C}]$ = aeroservoelastic output matrix for the balanced system (original time scale)
c = wing chord
$[C_A]$ = aerodynamic output matrix
$[\underset{\sim}{C}_d]$ = assembled damping matrix
$[\tilde{C}_d]$ = modal damping matrix
$[\hat{C}_d]$ = enhanced damping matrix
$[D]$ = aeroservoelastic feedthrough matrix using the original time scale
$[\tilde{D}]$ = aeroservoelastic feedthrough matrix using the recast time scale
$[\bar{D}]$ = aeroservoelastic feedthrough matrix for the balanced system (original time scale)
$[D_A^0]$ = aerodynamic feedthrough matrix corresponding to displacement input
$[D_A^1]$ = aerodynamic feedthrough matrix corresponding to velocity input
$[D_A^2]$ = aerodynamic feedthrough matrix corresponding to acceleration input
$\{\underset{\sim}{F}_{\text{act}}\}$ = assembled actuator force vector
$\{\tilde{F}_{\text{act}}\}$ = modal actuator force vector
$\{\underset{\sim}{F}_{\text{aero}}\}$ = assembled aerodynamic force vector
$\{\tilde{F}_{\text{aero}}\}$ = modal aerodynamic force vector
$[H]$ = solution to the recast controllability Lyapunov equation when $[\tilde{Q}]$ is equal to $[I]$
i = $\sqrt{-1}$
$[I]$ = identity matrix
$[\underset{\sim}{K}]$ = assembled stiffness matrix
$[\tilde{K}]$ = modal stiffness matrix
$[\hat{K}]$ = enhanced stiffness matrix
k = reduced frequency, $c/(2V_\infty) \times \omega$
$[k]$ = matrix of actuator rotational stiffnesses
$[\underset{\sim}{M}]$ = assembled mass matrix
$[\tilde{M}]$ = modal mass matrix
$[\hat{M}]$ = enhanced mass matrix
$\{\tilde{M}_{\text{act}}\}$ = modal actuator moment vector
N_l = number of aerodynamic lags used in Roger's rational function approximation (typically 0–3)
p = nondimensional Laplace variable related to reduced frequency $= ik$
$[Q]$ = matrix of aerodynamic influence coefficients in the frequency domain
$[\tilde{Q}]$ = $[\tilde{B}][\tilde{B}]^T$
q_∞ = freestream dynamic pressure
$[R]$ = matrix converting time scales
$[r]$ = transformation matrix from generalized deflection to control surface rotation
$[S]$ = arbitrary matrix
$\{s\}$ = generalized aeroservoelastic output using the recast time scale
$[T]$ = balancing transformation matrix using the original time scale
$[\tilde{T}]$ = balancing transformation matrix using the recast time scale
t = original time scale

Presented as Paper 2010-2947 at the 51st AIAA/ASME/ASCE/AHS/ASC Structures, Structural Dynamics, and Materials Conference, Orlando, FL, 12–15 April 2010; received 7 June 2010; revision received 1 October 2010; accepted for publication 4 October 2010.

*Senior Engineer, Research. Senior Member AIAA.
†Engineer, Research. Student Member AIAA.
‡Vice President of Engineering. Member AIAA.

V_∞ = freestream velocity
$\{v\}$ = eigenvector of $[A]$
$\{\tilde{v}\}$ = eigenvector of $[\tilde{A}]$
$[W_c]$ = controllability Gramian using the original time scale
$[\tilde{W}_c]$ = controllability Gramian using the recast time scale
$[W_o]$ = observability Gramian using the original time scale
$[\tilde{W}_o]$ = observability Gramian using the recast time scale
$\{x\}$ = arbitrary vector is not equal to $\{0\}$
$\{y\}$ = vector of nodal displacements/rotations (output from aeroservoelastic state-space system)
$\{z\}$ = vector of aerodynamic lag states
α = time scale conversion factor from the original to the recast time scale
β = time scale conversion factor for the aeroservoelastic output matrix
β^l = curve fit term corresponding to aerodynamic lag term l in Roger's rational function approximation
$\{\delta\}$ = vector of control surface rotations
$[\Delta A]$ = perturbation in $[A]$
$[\Delta \tilde{A}]$ = perturbation in $[\tilde{A}]$
$[\Delta B]$ = perturbation in $[B]$
$[\Delta \tilde{B}]$ = perturbation in $[\tilde{B}]$
$[\Delta Q]$ = perturbation in $[Q]$
$[\Delta \tilde{W}_c]$ = perturbation in $[\tilde{W}_c]$
$\{\delta_{\text{cmd}}\}$ = vector of commanded control surface rotations
ϵ_c = normalized error measure in computing the recast controllability Lyapunov equation
ϵ_o = normalized error measure in computing the recast observability Lyapunov equation
λ = eigenvalue of $[A]$
$\tilde{\lambda}$ = eigenvalue of $[\tilde{A}]$
$\{\xi\}$ = modal displacement vector
$[\sigma^2]$ = diagonal matrix of eigenvalues for balancing transformation using the original time scale
$[\tilde{\sigma}^2]$ = diagonal matrix of eigenvalues for balancing transformation using the recast time scale
τ = recast time scale
$[\Phi]$ = matrix of modal eigenvectors
$\{\phi\}$ = modal eigenvector
ω = natural frequency

I. Introduction

THE design of modern flight vehicles requires sophisticated mathematical models. Aeroservoelastic models combine aerodynamics, controls, and structural models into a single model that can be used for control law design. The importance of performing active control for flutter suppression, gust load alleviation, and ride quality enhancement was identified during the NASA High-Speed Research Program [1,2]. The design of control laws for this class of vehicles continues [3]. Ultimately, state-space models are required.

The size of such aeroservoelastic models can be quite large (on the order of thousands of states [4]) and thus unsuitable for control law design. One approach for reduction is computation of a balanced realization followed by truncation of the least important states. The balanced realization applied in the present research involves computing the controllability and observability Gramians of the aeroservoelastic model. Once these Gramians are computed, an eigenvalue problem is solved for the transformation matrix that results in the balanced states being ordered in terms of their controllability and observability [5–7]. It is in this stage that the truncation may be performed safely by eliminating the modes with the least controllability and observability.

Previous research has developed aeroservoelastic reduced-order models (ROMs) that are appropriate for control law design [4]. In this previous research, the Gramians needed for the balancing transformation were computed from the Lyapunov equations using the algorithm given in [8], which implements the Bartels–Stewart algorithm [9] using only real arithmetic. For the particular form of the aeroservoelastic state-space model implemented in [4], using a time scale of seconds was found to produce diverse entries in the state matrix that in turn led to relatively large errors in the solution of the Lyapunov equations.

In the present work, the time scale in the previously developed ROMs is changed in order to better condition the Lyapunov equations used to compute the Gramians. However, in order to avoid problems associated with new units for the physical dimension of time, the original system is the one that is balanced and truncated. For instance, seconds are the usual units of time, but better conditioning may be achieved using milliseconds as the time unit. In such a case, one would not want to archive the balanced and truncated version of the new system that uses milliseconds as the time unit. Rather, it is much better to store the balanced and truncated form of the original system that uses seconds as the time unit.

II. Original Linear Time Invariant System of Equations

The aeroservoelastic state-space model is generated using the methodology presented in [4]. A brief summary of this work is presented here.

A. Structural Model

The modal equations of motion are given as

$$[\tilde{M}]\{\ddot{\tilde{\xi}}\} + [\tilde{C}_d]\{\dot{\tilde{\xi}}\} + [\tilde{K}]\{\tilde{\xi}\} = \{\tilde{F}_{\text{aero}}\} + \{\tilde{F}_{\text{act}}\} \tag{1}$$

The following set of equations are used to compute the structural modal mass, stiffness, and damping matrices from the corresponding assembled finite element matrices:

$$[\tilde{M}] = [\Phi]^T[M][\Phi] \tag{2}$$

$$[\tilde{C}_d] = [\Phi]^T[C_d][\Phi] \tag{3}$$

$$[\tilde{K}] = [\Phi]^T[K][\Phi] \tag{4}$$

where $[\Phi]$ is computed from the generalized eigenvalue problem,

$$[K]\{\phi\} = \omega^2[M]\{\phi\} \tag{5}$$

and the modal forces are computed from the assembled forces as follows:

$$\{\tilde{F}_{\text{act}}\} = [\Phi]^T\{F_{\text{act}}\} \tag{6}$$

$$\{\tilde{F}_{\text{aero}}\} = [\Phi]^T\{F_{\text{aero}}\} \tag{7}$$

B. Aerodynamic Model

The doublet-lattice method is used to generate a potential flow solution to the unsteady system aerodynamics [10,11] in the frequency domain. Roger's rational function approximation (RFA) method [12] is used to obtain a state-space representation of the unsteady aerodynamics in the time domain. This is obtained in the classical manner by solving a curve fit to the generalized aerodynamic influence coefficients.

The unsteady aerodynamic data are converted to state-space form in the time domain using a RFA [12], giving

$$[Q(p)] = [A^0] + p[A^1] + p^2[A^2] + \sum_{l=1}^{N_l} \frac{p[B^l]}{p + \beta^l} \tag{8}$$

When converted into the time domain, the Laplace domain model becomes a state-space model of the form

$$\{\dot{z}\} = [A_A]\{z\} + [\,0 \quad B_A^1 \quad 0\,]\begin{Bmatrix}\xi\\ \dot{\xi}\\ \ddot{\xi}\end{Bmatrix} \tag{9}$$

and

$$\frac{1}{q_\infty}\{\tilde{F}_{\text{aero}}\} = [C_A]\{z\} + [\,D_A^0 \quad D_A^1 \quad D_A^2\,]\begin{Bmatrix}\xi\\ \dot{\xi}\\ \ddot{\xi}\end{Bmatrix} \tag{10}$$

Here, the aerodynamic state-space matrices are determined from the terms in Eq. (8) as follows:

$$[A_A] = \frac{2V_\infty}{c}\,\text{diag}(-\beta^1, -\beta^2, \ldots, -\beta^{N_l}) \tag{11}$$

$$[B_A^1] = \begin{bmatrix}\hat{B}_A & 0 & 0\\ 0 & \ddots & 0\\ 0 & 0 & \hat{B}_A\end{bmatrix} \tag{12}$$

$$[C_A] = [\,B^1 \quad B^2 \quad \cdots \quad B^{N_l}\,] \tag{13}$$

$$[D_A^0] = [A^0] \tag{14}$$

$$[D_A^1] = \frac{c}{2V_\infty}[A^1] \tag{15}$$

$$[D_A^2] = \left(\frac{c}{2V_\infty}\right)^2[A^2] \tag{16}$$

C. Actuator Model

In addition to modeling the structure and aerodynamics, an actuator model is included in the aeroservoelastic state-space model. This is done by modeling the actuator as a feedback control system. The actuator moment can be written as

$$\{\tilde{M}_{\text{act}}\} = [k](\{\delta_{\text{cmd}}\} - \{\delta\} - [a]\{\dot{\delta}\}) = [r]\{\tilde{F}_{\text{act}}\} \tag{17}$$

where the control surface deflections are given in terms of the generalized deflections as follows:

$$\{\delta\} = [r]\{\xi\} \tag{18}$$

Hence, the modal actuator forces are given by

$$\{\tilde{F}_{\text{act}}\} = [r]^T[k](\{\delta_{\text{cmd}}\} - [r]\{\xi\} - [a][r]\{\dot{\xi}\}) \tag{19}$$

D. Aeroservoelastic State-Space Model

The aeroservoelastic model is formed by combining Eqs. (1), (9), (10), and (19) together and writing them in state-space form. Considering acceleration to be the output, the result is given as follows:

$$\begin{Bmatrix}\dot{\xi}\\ \ddot{\xi}\\ \dot{z}\end{Bmatrix} = \begin{bmatrix}0 & I & 0\\ -\hat{M}^{-1}\hat{K} & -\hat{M}^{-1}\hat{C}_d & q_\infty\hat{M}^{-1}C_A\\ 0 & B_A^1 & A_A\end{bmatrix}\begin{Bmatrix}\xi\\ \dot{\xi}\\ z\end{Bmatrix} + \begin{bmatrix}0\\ \hat{M}^{-1}r^Tk\\ 0\end{bmatrix}\{\delta_{\text{cmd}}\} \tag{20}$$

and

$$\{\ddot{y}\} = [\,-\Phi\hat{M}^{-1}\hat{K} \quad -\Phi\hat{M}^{-1}\hat{C}_d \quad q_\infty\Phi\hat{M}^{-1}C_A\,]\begin{Bmatrix}\xi\\ \dot{\xi}\\ z\end{Bmatrix} + [\Phi\hat{M}^{-1}r^Tk]\{\delta_{\text{cmd}}\} \tag{21}$$

where the dot refers to time derivatives taken with respect to the original time scale t. The matrices $[\hat{M}]$, $[\hat{C}_d]$, and $[\hat{K}]$ are given by

$$[\hat{M}] = [\tilde{M}] - q_\infty[D_A^2] \tag{22}$$

$$[\hat{C}_d] = [\tilde{C}_d] - q_\infty[D_A^1] + [r]^T[k][a][r] \tag{23}$$

$$[\hat{K}] = [\tilde{K}] - q_\infty[D_A^0] + [r]^T[k][r] \tag{24}$$

The system of state-space equations is written in compact notation as follows:

$$\begin{Bmatrix}\dot{\xi}\\ \ddot{\xi}\\ \dot{z}\end{Bmatrix} = [A]\begin{Bmatrix}\xi\\ \dot{\xi}\\ z\end{Bmatrix} + [B]\{\delta_{\text{cmd}}\} \tag{25}$$

and

$$\{\ddot{y}\} = [C]\begin{Bmatrix}\xi\\ \dot{\xi}\\ z\end{Bmatrix} + [D]\{\delta_{\text{cmd}}\} \tag{26}$$

If, instead of acceleration, displacement is requested as the output, the set of linear output equations are given by

$$\{y\} = [\,\Phi \quad 0 \quad 0\,]\begin{Bmatrix}\xi\\ \dot{\xi}\\ z\end{Bmatrix} = [C]\begin{Bmatrix}\xi\\ \dot{\xi}\\ z\end{Bmatrix} \tag{27}$$

Likewise, if velocity is desired as the output, the linear output equations are given by

$$\{\dot{y}\} = [\,0 \quad \Phi \quad 0\,]\begin{Bmatrix}\xi\\ \dot{\xi}\\ z\end{Bmatrix} = [C]\begin{Bmatrix}\xi\\ \dot{\xi}\\ z\end{Bmatrix} \tag{28}$$

This system of equations potentially has conditioning problems regardless of the output. For instance, if

$$[\hat{M}^{-1}\hat{K}]_{ij} \gg 1 \quad \text{for some } i, j \tag{29}$$

then the resulting system of equations is likely ill-conditioned and the Gramian calculations will likely be in error. To overcome this problem, the time dimension of the state-space model is changed appropriately for use in computing the controllability and observability Gramians.

III. Recast System of Equations

To achieve better conditioning for computing the Gramians, the original time scale t is converted to a different time scale τ, where

$$\tau = \alpha t \tag{30}$$

For instance, if t is in seconds, choosing $\alpha = 1000$ ms/s gives τ in milliseconds. The first-order time derivatives in Eqs. (20) and (21) are transformed as follows:

$$\frac{\mathrm{d}\xi}{\mathrm{d}t} = \frac{\mathrm{d}\xi}{\mathrm{d}\left(\frac{1}{\alpha}\tau\right)} = \alpha\frac{\mathrm{d}\xi}{\mathrm{d}\tau} \tag{31}$$

and

$$\frac{\mathrm{d}z}{\mathrm{d}t} = \frac{\mathrm{d}z}{\mathrm{d}(\frac{1}{\alpha}\tau)} = \alpha\frac{\mathrm{d}z}{\mathrm{d}\tau} \tag{32}$$

Likewise, the second-order time derivative becomes

$$\frac{\mathrm{d}^2\xi}{\mathrm{d}t^2} = \frac{\mathrm{d}}{\mathrm{d}(\frac{1}{\alpha}\tau)}\left(\frac{\mathrm{d}\xi}{\mathrm{d}t}\right) = \alpha^2\frac{\mathrm{d}^2\xi}{\mathrm{d}\tau^2} \tag{33}$$

Letting $(\cdot)' = \mathrm{d}(\cdot)/\mathrm{d}\tau$, we have

$$\begin{Bmatrix}\xi\\ \dot{\xi}\\ z\end{Bmatrix} = \begin{bmatrix}I & 0 & 0\\ 0 & \alpha I & 0\\ 0 & 0 & I\end{bmatrix}\begin{Bmatrix}\xi\\ \xi'\\ z\end{Bmatrix} = [R]\begin{Bmatrix}\xi\\ \xi'\\ z\end{Bmatrix} \tag{34}$$

and

$$\begin{Bmatrix}\dot{\xi}\\ \ddot{\xi}\\ \dot{z}\end{Bmatrix} = \begin{bmatrix}\alpha I & 0 & 0\\ 0 & \alpha^2 I & 0\\ 0 & 0 & \alpha I\end{bmatrix}\begin{Bmatrix}\xi'\\ \xi''\\ z'\end{Bmatrix} = \alpha[R]\begin{Bmatrix}\xi'\\ \xi''\\ z'\end{Bmatrix} \tag{35}$$

Incorporating the change in the time scale, the state-space system of equations become

$$\begin{Bmatrix}\xi'\\ \xi''\\ z'\end{Bmatrix} = \frac{1}{\alpha}[R]^{-1}[A][R]\begin{Bmatrix}\xi\\ \xi'\\ z\end{Bmatrix} + \frac{1}{\alpha}[R]^{-1}[B]\{\delta_{\mathrm{cmd}}\} \tag{36}$$

$$= [\tilde{A}]\begin{Bmatrix}\xi\\ \xi'\\ z\end{Bmatrix} + [\tilde{B}]\{\delta_{\mathrm{cmd}}\} \tag{37}$$

and

$$\{s\} = \frac{1}{\beta}[C][R]\begin{Bmatrix}\xi\\ \xi'\\ z\end{Bmatrix} + [D]\{\delta_{\mathrm{cmd}}\} \tag{38}$$

$$= [\tilde{C}]\begin{Bmatrix}\xi\\ \xi'\\ z\end{Bmatrix} + [\tilde{D}]\{\delta_{\mathrm{cmd}}\} \tag{39}$$

where

$$\{s\} = \begin{cases}\{y\} & \text{displacement output}\\ \{y'\} & \text{velocity output}\\ \{y''\} & \text{acceleration output}\end{cases} \tag{40}$$

and

$$\beta = \begin{cases}1 & \text{displacement output}\\ \alpha & \text{velocity output}\\ \alpha^2 & \text{acceleration output}\end{cases} \tag{41}$$

Considering the acceleration to be the requested output, the system of state-space equations can be written explicitly as

$$\begin{Bmatrix}\xi'\\ \xi''\\ z'\end{Bmatrix} = \begin{bmatrix}0 & I & 0\\ -\frac{1}{\alpha^2}\hat{M}^{-1}\hat{K} & -\frac{1}{\alpha}\hat{M}^{-1}\hat{C}_d & \frac{q_\infty}{\alpha^2}\hat{M}^{-1}C_A\\ 0 & B_A^1 & \frac{1}{\alpha}A_A\end{bmatrix}\begin{Bmatrix}\xi\\ \xi'\\ z\end{Bmatrix} + \begin{bmatrix}0\\ \frac{1}{\alpha^2}\hat{M}^{-1}r^Tk\\ 0\end{bmatrix}\{\delta_{\mathrm{cmd}}\} \tag{42}$$

and

$$\{y''\} = \begin{bmatrix}-\frac{1}{\alpha^2}\Phi\hat{M}^{-1}\hat{K} & -\frac{1}{\alpha}\Phi\hat{M}^{-1}\hat{C}_d & \frac{q_\infty}{\alpha^2}\Phi\hat{M}^{-1}C_A\end{bmatrix}\begin{Bmatrix}\xi\\ \xi'\\ z\end{Bmatrix} + \left[\frac{1}{\alpha^2}\Phi\hat{M}^{-1}r^Tk\right]\{\delta_{\mathrm{cmd}}\} \tag{43}$$

If, however, displacement or velocity is desired, the output equation, respectively, becomes

$$\{y\} = [\,\Phi \quad 0 \quad 0\,]\begin{Bmatrix}\xi\\ \xi'\\ z\end{Bmatrix} \tag{44}$$

or

$$\{y'\} = [\,0 \quad \Phi \quad 0\,]\begin{Bmatrix}\xi\\ \xi'\\ z\end{Bmatrix} \tag{45}$$

IV. System Stability

In the present section, the intuitively obvious fact that the stability classification of the system is unaffected by changing the time scale will be shown mathematically. Recall that the stability of the unscaled system is obtained by examining the eigenvalues of $[A]$. If all of the eigenvalues of $[A]$ have negative real parts, the system is stable. The relevant eigenvalue problems for the unscaled and time-scaled systems, respectively, are

$$[A]\{v\} = \lambda\{v\} \tag{46}$$

and

$$[\tilde{A}]\{\tilde{v}\} = \tilde{\lambda}\{\tilde{v}\} \tag{47}$$

Using the definition of $[\tilde{A}]$, Eq. (47) can be recast as

$$[A][R]\{\tilde{v}\} = \alpha\tilde{\lambda}[R]\{\tilde{v}\} \tag{48}$$

Comparing Eqs. (46) and (48), the following results are observed:

$$\tilde{\lambda} = \frac{1}{\alpha}\lambda \tag{49}$$

and

$$\{\tilde{v}\} = [R]^{-1}\{v\} \tag{50}$$

Hence, it is clear that the eigenvalues of $[\tilde{A}]$ are simply the eigenvalues of $[A]$ scaled by factor $1/\alpha$. Therefore, if the original system is stable, the system with the recast time scale will also be stable, because only nonzero positive α values are allowed. Likewise, if the original

system is unstable, the recast system will also be unstable. Nevertheless, the margins of stability are affected, as the eigenvalues grow or shrink depending on α. For $\alpha > 1$, the eigenvalues of $[\tilde{A}]$ not only become smaller but also move closer together, even though the ratio of any one eigenvalue to any other particular eigenvalue remains constant.

V. Controllability and Observability Gramians

The original system of equations has a controllability Gramian, $[W_c]$, which satisfies the following Lyapunov equation:

$$[A][W_c] + [W_c][A]^T + [B][B]^T = [0] \tag{51}$$

and an observability Gramian, $[W_o]$, which satisfies the following Lyapunov equation:

$$[A]^T[W_o] + [W_o][A] + [C]^T[C] = [0] \tag{52}$$

Likewise, the recast system of equations have Gramians that identically satisfy

$$[\tilde{A}][\tilde{W}_c] + [\tilde{W}_c][\tilde{A}]^T + [\tilde{B}][\tilde{B}]^T = [0] \tag{53}$$

and

$$[\tilde{A}]^T[\tilde{W}_o] + [\tilde{W}_o][\tilde{A}] + [\tilde{C}]^T[\tilde{C}] = [0] \tag{54}$$

Substituting expressions for $[\tilde{A}]$ and $[\tilde{B}]$ into Eq. (53) gives

$$\frac{1}{\alpha}[R]^{-1}[A][R][\tilde{W}_c] + \frac{1}{\alpha}[\tilde{W}_c][R][A]^T[R]^{-1} + \frac{1}{\alpha^2}[R]^{-1}[B][B]^T[R]^{-1} = [0] \tag{55}$$

The final result of this equation is obtained by multiplying through by α^2 and premultiplying and postmultiplying each term by $[R]$ to give

$$\alpha[A][R][\tilde{W}_c][R] + \alpha[R][\tilde{W}_c][R][A]^T + [B][B]^T = [0] \tag{56}$$

Comparing Eq. (56) to Eq. (51) allows $[\tilde{W}_c]$ to be identified as

$$[\tilde{W}_c] = \frac{1}{\alpha}[R]^{-1}[W_c][R]^{-1} \tag{57}$$

The corresponding equation for the recast observability matrix is determined similarly and is given by

$$[\tilde{W}_o] = \frac{\alpha}{\beta^2}[R][W_o][R] \tag{58}$$

where β is given by Eq. (41).

VI. Balanced Realization

The goal in the present research is not only to convert the time scale for well-conditioned computation of the Gramians but also to balance and transform the original system of equations in order to prevent errors from being introduced due to inconvenient and inconsistent units being used for the time scale. That is, the reduced state-space model is meant to be created in a form suitable for easy use later. For instance, it may be necessary to use $\alpha = 1000$ ms/s for the computation of the Gramians, which means the time scale is in units of milliseconds if the original time unit is seconds. However, for archival purposes, it is much better to store the ROM with time units of seconds. That this can be easily achieved is demonstrated as follows.

The eigenvalue problem used to compute the transformation matrix for conventional balanced realization is determined for the original state-space system as

$$[W_c][W_o][T] = [T][\sigma^2] \tag{59}$$

where $[\sigma]$ is a diagonal matrix of eigenvalues. The corresponding equation for the recast system is given by

$$[\tilde{W}_c][\tilde{W}_o][\tilde{T}] = [\tilde{T}][\tilde{\sigma}^2] \tag{60}$$

That these two equations define equivalent eigenvalue problems is observed by substituting Eqs. (57) and (58) into Eq. (60) and simplifying to give

$$[W_c][W_o][R][\tilde{T}] = [R][\tilde{T}][\beta^2\tilde{\sigma}^2] \tag{61}$$

Hence,

$$[\tilde{\sigma}^2] = \left[\frac{1}{\beta^2}\sigma^2\right] \tag{62}$$

and

$$[R][\tilde{T}] = [T] \tag{63}$$

or

$$[\tilde{T}] = [R]^{-1}[T] \tag{64}$$

Equations (53) and (54) are solved for the Gramians corresponding to the recast system of equations. Then, the eigenvalue problem given by Eq. (60) is solved. Finally, the original set of state-space equations are transformed and truncated using $[T]$, determined from Eq. (63). That is, once $[T]$ has been calculated, the generalized balanced realization of the state-space matrices are determined as

$$[\bar{A}] = [T]^{-1}[A][T] \tag{65}$$

$$[\bar{B}] = [T]^{-1}[B] \tag{66}$$

$$[\bar{C}] = [C][T] \tag{67}$$

$$[\bar{D}] = [D] \tag{68}$$

Note that the resulting system involving $[\bar{A}]$, $[\bar{B}]$, $[\bar{C}]$, and $[\bar{D}]$ employs the original time scale units. Hence, the effects of changing the time scale do not affect the final state-space representation that is achieved. Rather, time scaling allows the balancing transformation to be computed using a better conditioned, albeit temporary, state-space representation.

VII. Gramian Calculation for the Recast System

The Gramians are computed directly using the methodology presented in [8]. Essentially, in this method, the Schur decompositions of $[\tilde{A}]$ and $[\tilde{A}]^T$ are employed to transform the controllability and observability Lyapunov equations into a more manageable form. The reader is directed to [8] for a complete discussion of the algorithm details.

VIII. Sensitivity of the Controllability Lyapunov Equation

To compare the sensitivity of the recast system to the original system, the sensitivity measure of [13] is applied to the controllability Lyapunov equations given by Eqs. (51) and (53). Let Eq. (53) be rewritten as

$$[\tilde{A}][\tilde{W}_c] + [\tilde{W}_c][\tilde{A}]^T + [\tilde{Q}] = [0] \tag{69}$$

Stable real systems with perturbations $[\Delta\tilde{A}]$, $[\Delta\tilde{W}_c]$, and $[\Delta\tilde{Q}]$ are considered with

$$([\tilde{A}] + [\Delta\tilde{A}])([\tilde{W}_c] + [\Delta\tilde{W}_c]) + ([\tilde{W}_c] + [\Delta\tilde{W}_c])([\tilde{A}] + [\Delta\tilde{A}])^T + ([\tilde{Q}] + [\Delta\tilde{Q}]) = [0] \tag{70}$$

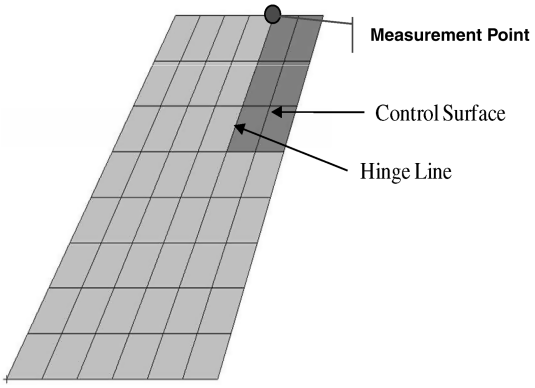

Fig. 1 Simple wing geometry. The single measurement point at the wingtip is labeled.

Let $[\tilde{H}]$ be the solution to Eq. (69) for the case when $[\tilde{Q}] = [I]$. That is,

$$[\tilde{A}][\tilde{H}] + [\tilde{H}][\tilde{A}]^T + [I] = [0] \tag{71}$$

The sensitivity measure is then

$$\frac{\|[\Delta\tilde{W}_c]\|_2}{\|[\tilde{W}_c] + [\tilde{\Delta}W_c]\|_2} \le 2\|[\tilde{A}] + [\Delta\tilde{A}]\|_2\|[\tilde{H}]\|_2\left[\frac{\|[\Delta\tilde{A}]\|_2}{\|[\tilde{A}] + [\Delta\tilde{A}]\|_2} + \frac{\|[\Delta\tilde{Q}]\|_2}{\|[\tilde{Q}] + [\Delta\tilde{Q}]\|_2}\right] \tag{72}$$

where $\|\cdot\|_2$ represents the spectral or two-norm, which is defined as

$$\|[S]\|_2 = \max\frac{\|[S]\{x\}\|_2}{\|\{x\}\|_2} \tag{73}$$

with

$$\|\{x\}\|_2 = \sqrt{\{x\}^T\{x\}} \neq 0 \tag{74}$$

In Eq. (72), it is assumed that $\|[\tilde{A}] + [\Delta\tilde{A}]\|_2$, $\|[\tilde{W}_c] + [\Delta\tilde{W}_c]\|_2$, and $\|[\tilde{Q}] + [\Delta\tilde{Q}]\|_2$ are all nonzero. Equation (72) is written in compact notation as

$$\text{LHS} \le \text{RHS} \tag{75}$$

where LHS denotes left-hand side and RHS denotes right-hand side.

IX. Selection of Time Scale Conversion Factor

The selection of α is problem dependent. However, a large range of acceptable values for α likely exists for most problems. To find an acceptable value for α in a quantifiable manner, it is beneficial to compute normalized error measures for the controllability and observability Lyapunov equations. These are defined as follows:

$$\epsilon_c \equiv \frac{\|[\tilde{A}][\tilde{W}_c] + [\tilde{W}_c][\tilde{A}]^T + [\tilde{B}][\tilde{B}]^T\|_F}{\|[\tilde{A}]\|_F} \tag{76}$$

and

$$\epsilon_o \equiv \frac{\|[\tilde{A}]^T[\tilde{W}_o] + [\tilde{W}_o][\tilde{A}] + [\tilde{C}]^T[\tilde{C}]\|_F}{\|[\tilde{A}]\|_F} \tag{77}$$

where $\|\cdot\|_F$ represents the Frobenius norm, which is defined as follows for real matrices:

$$\|[S]\|_F = \sqrt{\sum_{i=1}^{m}\sum_{j=1}^{n}|S_{ij}|^2} = \sqrt{\text{trace}([S]^T[S])} \tag{78}$$

It should be clear that, in the case of an exact calculation of the Gramians for the recast system, the numerators in Eqs. (76) and (77) will be zero. The goal is to select an α value that gives normalized error measures as low as possible. The process for finding an acceptable value of α is either based upon user experience or trial and error. Although a trial and error process may initially seem to be unsatisfactory from a computational standpoint, it should be noted that such a process does not involve recomputing either the structural or aerodynamic solutions. Rather, it is only necessary to rescale the resulting aeroservoelastic system according to Eqs. (42–45). The recast Gramians and the needed balancing transformations are then easily computed. Then one simply checks the relative errors in the recast controllability and observability Lyapunov equations to assure that both equations have been solved satisfactorily. On a modern personal computer, such a trial and error process is not computationally prohibitive.

X. Simple Wing Example Problem

The first example problem selected for this development is a simple wing with a control surface at the trailing edge. This configuration is shown in Fig. 1. A single measurement point at the wingtip is chosen to go along with the single input of the control surface deflection. The flight conditions consist of a Mach number of 0.3 and a dynamic pressure of 200 psi.

A. Three-State Solution

For the purposes of demonstrating the effect of scaling on the system matrices, a single elastic mode along with a single aerodynamic lag state is used. This gives a total of three states that must be evaluated. The original system has the following $[A]$ and $[B]$ matrices:

$$[A] = \begin{bmatrix} 0 & 1 & 0 \\ -5.9409 \times 10^7/\text{s}^2 & -13,233.2/\text{s} & -1.1526 \times 10^6/\text{s}^2 \\ 0 & 1 & -6821.76/\text{s} \end{bmatrix} \tag{79}$$

and

$$[B] = \begin{bmatrix} 0 \\ -1.4939 \times 10^9/\text{s}^2 \\ 0 \end{bmatrix} \tag{80}$$

Using $\alpha = 1000$ ms/s gives a recast system where time is measured in milliseconds. The $[A]$ and $[B]$ matrices for the recast system are

$$[\tilde{A}] = \begin{bmatrix} 0 & 1 & 0 \\ -59.409/\text{ms}^2 & -13.2332/\text{ms} & -1.1526/\text{ms}^2 \\ 0 & 1 & -6.82176/\text{ms} \end{bmatrix} \tag{81}$$

and

$$[\tilde{B}] = \begin{bmatrix} 0 \\ -1493.9/\text{ms}^2 \\ 0 \end{bmatrix} \tag{82}$$

Considering displacement to be the output of interest, the following matrices complete the original and recast systems:

Table 1 Conditioning of the three-state system

α	LHS	RHS	cond($[\tilde{A}]$)	ϵ_c	ϵ_o
1.0	0.0099	7.907×10^9	5.9420×10^7	1.4551×10^6	7.4752×10^{-23}
1000.0	0.0099	8.7303	63.0554	2.4872×10^{-11}	3.0492×10^{-17}

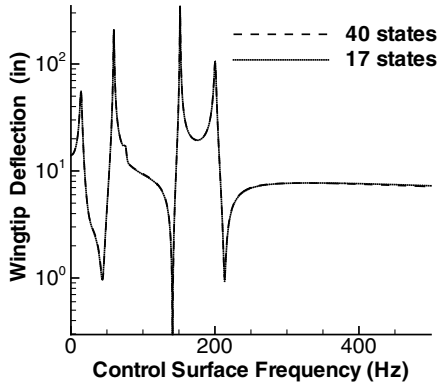

Fig. 2 Magnitude of the frequency response of the wingtip deflection as a function of the control surface frequency for the full and truncated systems.

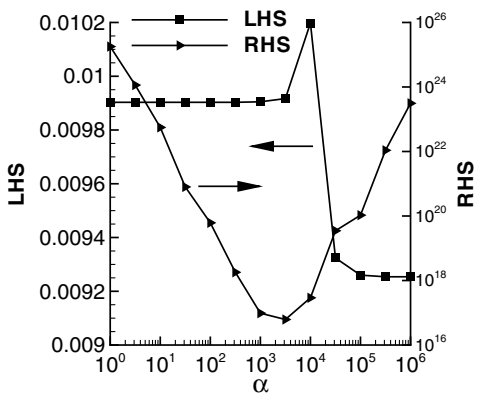

Fig. 3 Sensitivity of the 40-state system.

$$[C] = [\tilde{C}] = [\,\Phi \quad 0 \quad 0\,] \tag{83}$$

and

$$[D] = [\tilde{D}] = [0] \tag{84}$$

It is clear from inspection that the recast system is much better conditioned than the original system. Table 1 shows the values for the LHS and RHS of Eq. (72) for the controllability problem, considering all nonidentity entries in $[A]$ and $[B]$ to be altered by 1%. More specifically, $[A]$ and $[B]$ are modified, and the corresponding modifications to $[\tilde{A}]$ and $[\tilde{B}]$ are found using their definitions. That is,

$$[\Delta\tilde{A}] = \frac{1}{\alpha}[R]^{-1}[\Delta A][R] \tag{85}$$

and

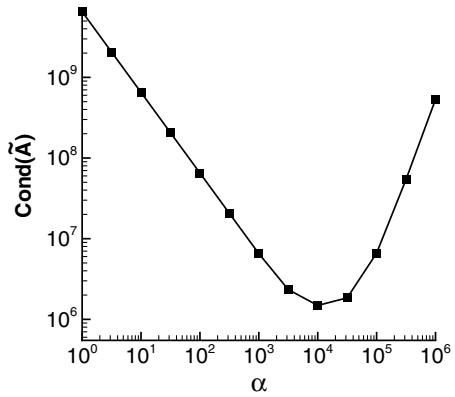

Fig. 4 Condition of $[\tilde{A}]$ for the 40-state system.

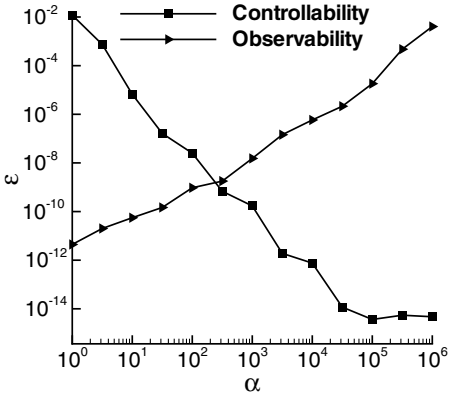

Fig. 5 Relative error in solving the Lyapunov equations for the 40-state system.

$$[\Delta\tilde{B}] = \frac{1}{\alpha}[R]^{-1}[\Delta B] \tag{86}$$

Note that the LHS of Eq. (72), which is the relative change in the controllability Gramian, is not exactly 0.01, because the identity entry is exact in $[A]$ and is left unmodified. The condition number of $[\tilde{A}]$ is also shown in Table 1, along with normalized error measures for the controllability and observability Lyapunov equations.

Although using the original system ($\alpha = 1$) along with the algorithm from [8] produces reasonably accurate results for the observability Gramian ($\epsilon_o \approx 0$), the results for the controllability Gramian are quite in error ($\epsilon_c \gg 0$). Using a time scale conversion factor of $\alpha = 1000$ ms/s produces controllability results that are much better behaved, while the observability results remain reasonably accurate. It is also noted that the bound on the relative change in the Gramian (RHS) decreases dramatically in going from $\alpha = 1$ to $\alpha = 1000$ ms/s.

B. Forty-State Solution

Here, a total of eight elastic modes and three aerodynamic lag states per elastic mode are used. The magnitude of the frequency response of the wingtip deflection as a function of the control surface excitation is shown in Fig. 2. Also shown in Fig. 2 is the magnitude of the frequency response for the balanced and truncated system, where 17 of the 40 possible states are used. As is evident from examining the figure, excellent results have been obtained from the balanced and truncated system.

Results for the LHS and RHS of Eq. (72) versus α are plotted in Fig. 3. It is noted that the bound provided by Eq. (72) is not very tight for this larger system, even when significant scaling is applied. Nevertheless, the bound appears to be best for a value of α near 10^3 ms/s.

The condition number of $[\tilde{A}]$ versus α is plotted in Fig. 4, and the relative errors in solving the Lyapunov equations for the Gramians are shown in Fig. 5. The condition of $[\tilde{A}]$ appears to be optimal near $\alpha = 10^4$. The errors in the controllability and observability Gramians

Fig. 6 S4T model.

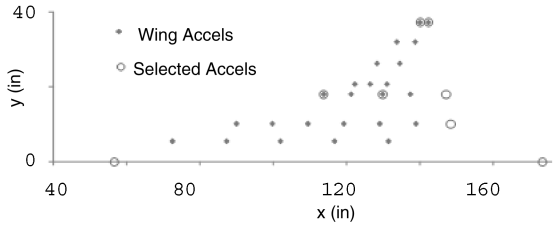

Fig. 7 Locations of selected accelerometers.

show opposite trends with α. Considering the controllability and observability Gramians equally, the optimal value appears to be near $\alpha = 200$. The final choice of α depends on the problem at hand. Nevertheless, there are large ranges in α that are acceptable.

XI. S4T Example Problem

The S4T configuration is a scaled version of a supersonic transport configuration (developed by NASA, The Boeing Company, and McDonnell Douglas Helicopter Systems) known as the technology concept aircraft (TCA). A photograph of the S4T model is shown in Fig. 6. This model is 192 in. (16 ft) long, representing a 4.91% scaled version of the TCA. The mass and stiffness of the model have been tailored to achieve dynamically scaled structural behavior [1]. The model is constructed with a graphite-epoxy flexible fuselage beam, a fiberglass-epoxy/honeycomb sandwich wing, and graphite-epoxy control surfaces. To represent the structural dynamics of the TCA fuselage, the flexible fuselage beam is mounted to a stiff aluminum channel through springs at four locations. This aluminum channel is referred to as the rigid beam and is connected through a balance to the wind-tunnel wall. The model has three actuated control surfaces, variable mass engine nacelles, and instrumentation to measure acceleration, strain, and pressure.

The S4T model is instrumented with 43 accelerometers, 6 strain gages, and 55 pressure taps. Based on the results of some open-loop testing, eight sensors are selected that have relatively high coherence and transfer magnitude at frequencies corresponding to the two lowest frequency modes. The accelerometers chosen for this study are shown in Fig. 7.

Actuation of the S4T model is addressed with three aerodynamic control surfaces. This includes a flap, a horizontal tail, and a ride control vane (RCV). The locations of these control surfaces are shown in Fig. 8.

The flight conditions are given by a Mach number of 0.8, a dynamic pressure of 0.277778 psi, and a flight velocity of

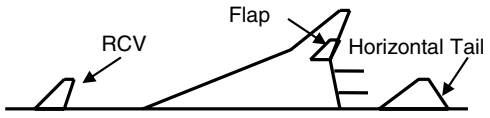

Fig. 8 Locations of control surfaces.

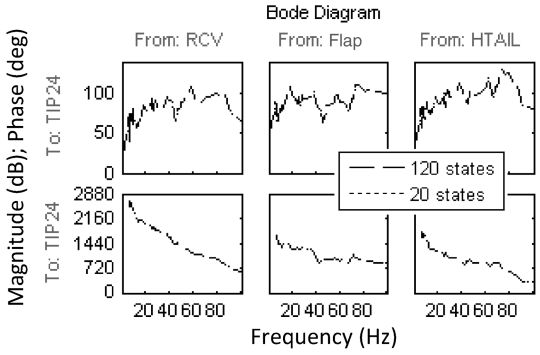

Fig. 9 Bode plots from the three inputs to the aft wingtip acceleration (HTAIL denotes horizontal tail).

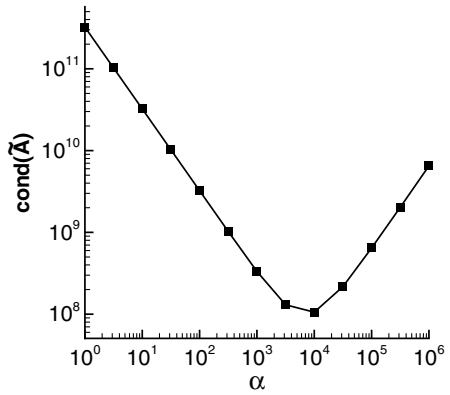

Fig. 10 Condition number of $[\tilde{A}]$ as a function of scaling parameter α for the 120 state solution.

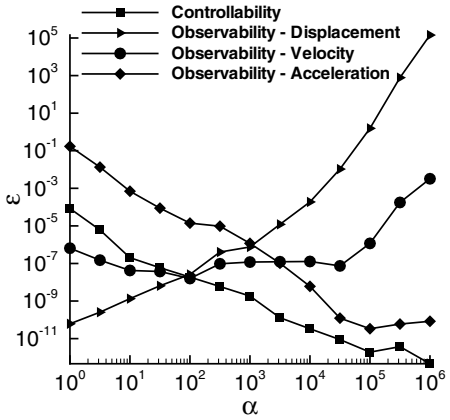

Fig. 11 Relative error in solving the Lyapunov equations for the Gramians of the 120-state system. Errors for the case where displacement, velocity, or acceleration are taken as the output are shown.

5079.0 in/s. The aerodynamics are represented using the doublet-lattice method. A total of 30 structural modes and two aerodynamic lags are used to represent the S4T model. This results in a total of 120 states to go along with the eight chosen outputs and three inputs. A total of 24 transfer functions exist, with a representative set shown in Fig. 9, for the acceleration of the aft wingtip point as a function of the RCV, flap, and horizontal tail inputs. Using the full 120 states or truncating to 20 states produces the same results.

The condition number of $[\tilde{A}]$ is shown in Fig. 10. Based on the condition number alone, the optimal time scaling appears to be $\alpha = 10^4$. The relative errors in calculating the Gramians from the Lyapunov equations [Eqs. (76) and (77)] are shown in Fig. 11. The relative error in calculating $[\tilde{W}_c]$ shows an overall downward trend with increasing α. Here, three separate error measures for the observability Gramian are computed based on whether the displacement, velocity, or acceleration are chosen as the output. Similar to the simple wing example, when displacement is chosen as the output, the controllability and observability errors have opposite trends with increasing α. The relative error in computing $[\tilde{W}_o]$ for acceleration output has a similar trend to that for $[\tilde{W}_c]$. Finally, the trend for ϵ_o for velocity output falls in between that for displacement and acceleration output. Considering displacement or velocity output, the optimal value (i.e., the value that weights ϵ_c and ϵ_o equally) appears to be $\alpha = 10^2$, whereas for acceleration output, an α of 10^5 minimizes ϵ_o.

Once again, even though the optimal value of α is not coincident when considering the condition number of $[\tilde{A}]$, ϵ_c, and ϵ_o, there appears to be a wide range of values that produce acceptable errors in calculating $[\tilde{W}_c]$ and $[\tilde{W}_o]$.

XII. Conclusions

A methodology for modifying the time scale in aeroservoelastic state-space equations has been presented. This time scale conversion leads to better-conditioned Lyapunov equations, which can be solved for controllability and observability Gramians. Subsequently, these Gramians can be used to create a balanced and truncated ROM in the original time units for archival purposes. The optimal value of the time scale conversion factor is problem- and output-dependent, but a large range of acceptable values likely exists for most problems. Because only the time scale of the assembled aeroservoelastic system is changed, it is not necessary to recompute the structural or aerodynamic solutions to find an acceptable value of the time scale conversion factor. Such a trial and error process to find an acceptable time scale is not computationally prohibitive, given even modest computational resources.

Acknowledgments

Funding for this development has been provided by the Aeroelasticity Branch of NASA Langley Research Center. The NASA technical representative for this research was Walter A. Silva.

References

[1] Baker, M., and Lenkey, P., "Parametric Flutter Analysis of the TCA Configuration and Recommendation for FFM Design and Scaling," The Boeing Co. Rept. CRAD-9408-TR-3342, Seattle, WA, 1997.

[2] Fogarty, T., and Baker, M., "MSC/NASTRAN Flutter Analysis of TCA with Lateral and Directional Control Laws," High-Speed Research Program Memorandum, The Boeing Co., Long Beach, CA, 1998.

[3] Perry, B., Silva, W.,Florance, J., Wieseman, C., Pototzky, A., Sanetrik, M., Scott, R., Keller, D., and Cole, S., "Plans and Status of Wind-Tunnel Testing Employing an Aeroservoelastic Semispan Model," 48th AIAA/ASME/ASCE/AHS/ASC Structures, Structural Dynamics, and Materials Conference, Honolulu, HI, AIAA Paper 2007-1770, 2007.

[4] Roughen, K. M., Bendiksen, O. O., and Baker, M. L., "Development of Generalized Aeroservoelastic Reduced Order Models," 50th AIAA/ASME/ASCE/AHS/ASC Structures, Structural Dynamics, and Materials Conference, Palm Springs, CA, AIAA Paper 2009-2491, 2009.

[5] Moore, B. C., "Principal Component Analysis in Linear Systems: Controllability, Observability, and Model Reduction," *IEEE Transactions on Automatic Control*, Vol. 26, No. 1, 1981, pp. 17–32. doi:10.1109/TAC.1981.1102568

[6] Laub, A., Heath, M., Paige, C., and Ward, R., "Computation of System Balancing Transformations and Other Applications of Simultaneous Diagonalization Algorithms," *IEEE Transactions on Automatic Control*, Vol. 32, No. 2, 1987, pp. 115–122. doi:10.1109/TAC.1987.1104549

[7] Tombs, M., and Postlethwaite, I., "Truncated Balanced Realization of a Stable Non-Minimal State-Space System," *International Journal of Control*, Vol. 46, No. 4, 1987, pp. 1319–1330. doi:10.1080/00207178708933971

[8] Sorensen, D., and Zhou, Y., "Direct Methods for Matrix Sylvester and Lyapunov Equations," *Journal of Applied Mathematics*, Vol. 2003, No. 6, 2003, pp. 277–303. doi:10.1155/S1110757X03212055.

[9] Bartels, R. M., and Stewart, G. W., "Algorithm 432: Solution of the Matrix Equation $AX + XB = C$," *Communications of the ACM*, Vol. 15, No. 9, 1972, pp. 820–826. doi:10.1145/361573.361582

[10] Giesing, J., Kalman, T., and Rodden, W., "Subsonic Unsteady Aerodynamics for General Configuration," Air Force Flight Dynamics Lab. TR 71-5, Wright-Patterson AFB, OH, 1971.

[11] Rodden, W., Harder, R., and Bellinger, E., "Aeroelastic Addition to NASTRAN," NASA CR 3094, 1979.

[12] Roger, K., "Airplane Math Modeling Methods for Active Control Design," *Structural Aspects of Active Controls*, AGARD CP 228, 1977.

[13] Hewer, G., and Kenney, C., "The Sensitivity of the Stable Lyapunov Equation," *SIAM Journal on Control and Optimization*, Vol. 26, No. 2, 1988, pp. 321–344. doi:10.1137/0326018